

## COMPTON SCATTERING IN THE KLEIN-NISHINA REGIME REVISITED

MASAAKI KUSUNOSE

Department of Physics, School of Science and Technology, Kwansei Gakuin University, Sanda 669-1337, Japan;  
kusunose@kwansei.ac.jp

AND

FUMIO TAKAHARA

Department of Earth and Space Science, Graduate School of Science, Osaka University, Toyonaka 560-0043, Japan;  
takahara@vega.ess.esi.osaka-u.ac.jp

Received 2004 August 3; accepted 2004 November 11

### ABSTRACT

In blazars such as 3C 279, GeV gamma rays are thought to be produced by inverse Compton scattering of soft photons injected from external sources into the jet. Because of the large bulk Lorentz factor of the jet, the energy of soft photons is Doppler shifted in the comoving frame of the jet, and the scattering is likely to occur in the Klein-Nishina regime. Although the Klein-Nishina effects are well known, the properties of the electron and emission spectra have not been studied in detail in the environment of blazars. We solve the kinetic equation of electrons with the spatial escape term of the electrons to obtain the electron energy spectrum in the jet and calculate the observed emission spectrum. In calculations of the Compton losses in the Klein-Nishina regime, we use the discrete loss formalism to take into account the significant energy loss in a single scattering. Although the scattering cross section decreases because of the Klein-Nishina effects, ample gamma rays are emitted by inverse Compton scattering. When the injection spectrum of electrons obeys a power law, the electron spectrum does not follow a broken power law, as a result of the Klein-Nishina effects, and a large number of high-energy electrons remain in the emitting region.

*Subject headings:* gamma rays: theory — radiation mechanisms: nonthermal

### 1. INTRODUCTION

Inverse Compton (IC) scattering is an important process in producing high-energy photons in astrophysical objects such as active galactic nuclei and gamma-ray bursts. Blazars are one of the important sites at which IC scattering is a major radiation process. The radiation from blazars is well described by synchrotron emission and IC scattering (e.g., Sikora et al. 1994; Inoue & Takahara 1996; Ghisellini et al. 1996). The spectral energy distribution of blazars has two peaks in the  $\nu\text{-}\nu F_\nu$  representation; one is in the range between IR and X-rays, and the other, in gamma rays such as GeV and TeV regions. The emission region of blazars is thought to be in the relativistic jet close to the central black hole, and the nonthermal electrons accelerated in the jet are probably responsible for the emission. Synchrotron radiation emitted by the nonthermal electrons produces the low-energy peak, and IC scattering by the same nonthermal electrons produces the high-energy peak. Although there are hadronic models that assume relativistic protons (e.g., Mücke et al. 2003), we confine ourselves to leptonic models, which assume radiation from nonthermal electrons/positrons alone.

In the jet of 3C 279, nonthermal electrons Compton scatter external soft photons to produce GeV gamma rays (Inoue & Takahara 1996); the source of the external soft photons may be accretion disks or broad-line regions (e.g., Dermer & Schlickeiser 1993; Sikora et al. 1994). In a previous paper (Kusunose et al. 2003), we showed that the electron spectrum in the emission region of 3C 279 does not obey a conventional broken power law, which appears if scattering occurs in the Thomson regime. The electron energy spectrum of 3C 279 is found to be harder than the broken power law in the high-energy region because of the Klein-Nishina (KN) effects.

When the electron Lorentz factor  $\gamma$  and the seed soft photon energy normalized by the electron rest mass  $x = h\nu/(m_e c^2)$  satisfy  $\gamma x < 1$ , IC scattering occurs in the Thomson regime. Here  $m_e$  and  $c$  are the electron rest mass and the speed of light, respectively. On the other hand, if  $\gamma x > 1$ , IC scattering occurs in the KN regime (e.g., Blumenthal & Gould 1970; Rybicki & Lightman 1979). In astrophysical objects high-energy radiation is often emitted by nonthermal electrons with a power-law distribution. In the objects in which nonthermal electrons are injected, radiate, and escape, the electron spectrum becomes steeper for  $\gamma > \gamma_{\text{br}}$ , where  $\gamma_{\text{br}}$  is the Lorentz factor determined by the balance between the Compton cooling and the electron escape, if the scattering occurs in the Thomson regime. When the injection spectrum obeys a power law,  $q_e(\gamma) \propto \gamma^{-p}$ , the steady state spectrum obeys a broken power law:  $n_e(\gamma) \propto \gamma^{-p}$  for  $\gamma < \gamma_{\text{br}}$  and  $n_e(\gamma) \propto \gamma^{-p-1}$  for  $\gamma > \gamma_{\text{br}}$ .

The effects of IC scattering in the KN regime have been studied by several authors. Blumenthal (1971), for example, showed that the electron spectrum becomes harder in the KN regime, assuming that monoenergetic soft photons are scattered. Zdziarski & Krolik (1993) demonstrated that when the electrons are injected with a power-law distribution with a power-law index of 2, the emission spectrum is flat in the  $\nu\text{-}\nu F_\nu$  representation if the KN effects are taken into account, although they assumed that the scattering cross section is zero for  $\gamma x > 3/4$  to simulate the KN effects. These properties were applied to the explanation of the TeV emission from Mrk 421 and its flat spectrum in the GeV–TeV region in the  $\nu\text{-}\nu F_\nu$  representation. Zdziarski (1989) solved kinetic equations for various types of injection spectra of electrons and soft photons, using the KN cross section.

In the above work (Blumenthal 1971; Zdziarski 1989), the electron escape from the emission region was not included. In

objects such as blazars, the emission region exists in the relativistically moving jets. Because the advection or adiabatic expansion of nonthermal particles removes the particles from the emission region on a timescale close to the light crossing time  $R/c$ , where  $R$  is the radius of the emission region, the effect of escaping particles on the spectra of electrons and photons is important. In this paper we show the properties of the spectra of electrons and photons when the electron escape is included and the scattering occurs predominantly in the KN regime. We also assume that synchrotron radiation is not important for radiative cooling; this is justified when ample soft photons from external sources are injected as seed photons of IC scattering.

In § 2 the kinetic equation of electrons is presented, and numerical results are given in § 3. Finally, we summarize our results in § 4.

## 2. KINETIC EQUATION

The kinetic equation for the steady state electrons is given by

$$-n_e(\gamma) \int_1^\gamma d\gamma' C(\gamma, \gamma') + \int_\gamma^\infty d\gamma' n_e(\gamma') C(\gamma', \gamma) + q_e(\gamma) - \frac{n_e(\gamma)}{t_{\text{esc}}} = 0, \quad (1)$$

where  $n_e(\gamma)$  is the number density of electrons per unit  $\gamma$ ,  $q_e(\gamma)$  is the injection rate of nonthermal electrons per unit volume and  $\gamma$ ,  $t_{\text{esc}}$  is the electron escape time, and  $C(\gamma, \gamma')$  describes the transition rate of an electron from  $\gamma$  to  $\gamma'$ . We assume that  $q_e(\gamma)$  is given by

$$q_e(\gamma) = q_0 \gamma^{-p} \exp(-\gamma/\gamma_{\text{max}}), \quad \gamma > \gamma_{\text{min}}, \quad (2)$$

where  $p$ ,  $\gamma_{\text{min}}$ ,  $\gamma_{\text{max}}$ , and  $q_0$  are parameters.

In scattering, the electron Lorentz factor  $\gamma$  decreases to  $\gamma'$ . When the number spectrum of soft photons per unit volume,  $n_{\text{soft}}(x)$ , is given, the rate of scattering ( $\gamma \rightarrow \gamma'$ ) per electron is given by Jones (1968; see also Zdziarski 1988) as

$$C(\gamma, \gamma') = \frac{3\sigma_{\text{T}}c}{4} \times \int_{E_*/\gamma}^\infty \frac{1}{E\gamma} \left[ r + (2-r) \frac{E_*}{E} - 2 \left( \frac{E_*}{E} \right)^2 - 2 \frac{E_*}{E} \ln \frac{E}{E_*} \right] n_{\text{soft}}(x) dx, \quad (3)$$

where

$$E = \gamma x, \quad E_* = \frac{\gamma/\gamma' - 1}{4}, \quad E > E_*, \quad r = \frac{1}{2} \left( \frac{\gamma}{\gamma'} + \frac{\gamma'}{\gamma} \right). \quad (4)$$

Here  $\sigma_{\text{T}}$  is the Thomson cross section, and we assume that the soft photons are isotropic. Equation (3) retains the zeroth-order term in a double expansion of the exact rate in  $1/\gamma^2$  and  $x/\gamma$ ; the exact cross section is given by Jones (1968; see also Coppi & Blandford 1990). Since we are interested in the KN regime, the above approximated cross section is enough to evaluate the electron spectrum for  $\gamma \gg 1$ . We assume that soft photons with energy  $x_s$  are isotropically distributed around the jet, where  $x_s$  is measured in the frame of the soft photon source. In the jet frame, the soft photon energy is Doppler shifted to  $x = \Gamma x_s$ , where  $\Gamma$  is

the bulk Lorentz factor of the jet. The radiation field is approximated to be isotropic in the jet frame for simplicity.

To solve equation (1), we discretize the equation as

$$-n_e(\gamma_i) \sum_{j=1}^{i-1} C(\gamma_i, \gamma_j) \gamma_j \Delta \ln \gamma + \sum_{j=i+1}^J n_e(\gamma_j) C(\gamma_j, \gamma_i) \gamma_j \Delta \ln \gamma + q_e(\gamma_i) - \frac{n_e(\gamma_i)}{t_{\text{esc}}} = 0, \quad (5)$$

where  $\gamma_i$  ( $i = 1, \dots, J$ ) is binned logarithmically and  $\Delta \ln \gamma = \ln \gamma_{i+1} - \ln \gamma_i$ , with  $\Delta \ln \gamma$  being constant (typically  $\Delta \ln \gamma = 2 \times 10^{-3}$ ). Here we omitted the term  $C(\gamma_i, \gamma_i)$ , because most electrons lose energy in scattering. We then obtain

$$n_e(\gamma_i) = A^{-1} \left[ \sum_{j=i+1}^J n_e(\gamma_j) C(\gamma_j, \gamma_i) \gamma_j \Delta \ln \gamma + q_e(\gamma_i) \right], \quad (6)$$

where

$$A = \sum_{j=1}^{i-1} C(\gamma_i, \gamma_j) \gamma_j \Delta \ln \gamma + \frac{1}{t_{\text{esc}}}. \quad (7)$$

We calculate  $n_e(\gamma_i)$  numerically from equation (6) with the upper boundary condition such that  $n_e(\gamma_J) = 0$ . Because  $C(\gamma, \gamma')$  in equation (3) is applicable to large values of  $\gamma$ , our numerical calculations are limited to  $\gamma_1 > \text{several}$ .

The injected electrons lose energy by IC scattering and move to the lower energy region in the energy space. The cooling rate of IC scattering is given by

$$\dot{\gamma} = \int_1^\gamma d\gamma' (\gamma' - \gamma) C(\gamma, \gamma'). \quad (8)$$

The cooling time is then defined as  $t_{\text{IC}}(\gamma) = \gamma/|\dot{\gamma}|$ . In the Thomson regime,  $t_{\text{IC}}(\gamma)$  decreases with increasing  $\gamma$  and attains a minimum value at  $\gamma \sim x_0^{-1}$ , where  $x_0$  is the characteristic energy of soft photons. For  $\gamma > x_0^{-1}$ , where the scattering occurs in the KN regime,  $t_{\text{IC}}(\gamma)$  increases.

Nonthermal particles in the jet may escape from the emission region by advection or diffusion, or adiabatic expansion effectively removes them. Because of the lack of knowledge on the electron escape time,  $t_{\text{esc}}$  is assumed to be independent of  $\gamma$  and given by  $t_{\text{esc}} = \zeta_{\text{esc}} \min\{t_{\text{IC}}(\gamma)\}$ , where  $\zeta_{\text{esc}}$  is a parameter and  $\min\{t_{\text{IC}}(\gamma)\}$  is the minimum value of  $t_{\text{IC}}(\gamma)$ , which is taken at  $\gamma \sim x_0^{-1}$ .

For comparison with the scattering in the KN regime, we also calculate the electron spectrum derived with the Thomson approximation. The kinetic equation of electrons in the Thomson regime is given by

$$\frac{d}{d\gamma} [\dot{\gamma}_{\text{T}}(\gamma) n_e(\gamma)] = q_e(\gamma) - \frac{n_e(\gamma)}{t_{\text{esc}}}, \quad (9)$$

where the cooling rate is calculated as (Lightman & Zdziarski 1987)

$$\dot{\gamma}_{\text{T}}(\gamma) = -\sigma_{\text{T}}c \left( \frac{4}{3} \gamma^2 - 1 \right) \int_0^{3/(4\gamma)} n_{\text{soft}}(x) x dx. \quad (10)$$

Here the scattered photon energy  $x'$  is assumed to be given by  $x' = (4/3)\gamma^2 x$ , and the scattering cross section is assumed to

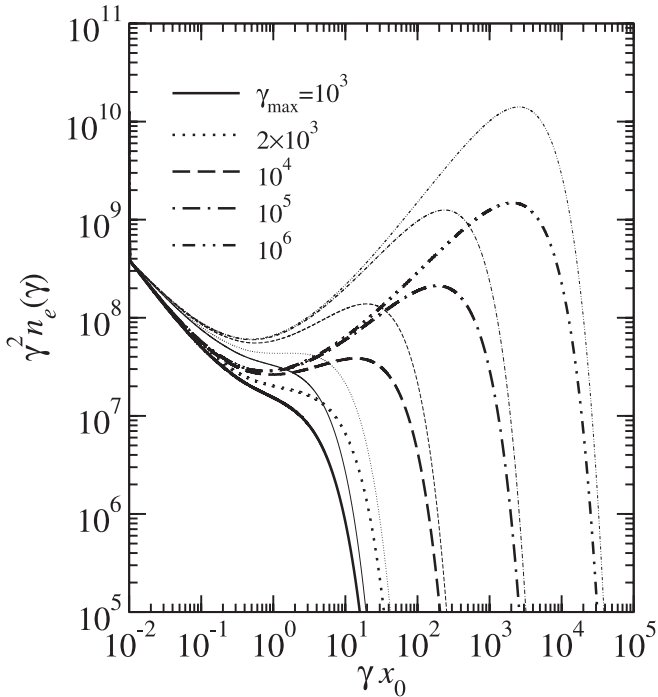


FIG. 1.—Electron spectra for various values of  $\gamma_{\max}$  without particle escape from the emission region. Thick and thin lines are for  $p = 2$  and  $1.8$ , respectively. The injection of monochromatic soft photons with  $m_e c^2 x_0 = 1.25$  keV is assumed. The KN effects are apparent for  $\gamma x_0 \gtrsim 0.1$ .

be zero for  $x\gamma > 3/4$  to simulate the scattering in the KN regime. The solution of equation (9) is given by

$$n_e(\gamma) = -\frac{1}{\dot{\gamma}_T(\gamma)} \int_{\gamma}^{\infty} q_e(\xi) \exp\left[\frac{1}{t_{\text{esc}}} \int_{\gamma}^{\xi} \frac{d\eta}{\dot{\gamma}_T(\eta)}\right] d\xi. \quad (11)$$

### 3. NUMERICAL RESULTS

We solve equation (1) numerically to obtain the electron spectrum and calculate the emission spectrum. The emission region is assumed to be in a relativistically moving blob, and we calculate the emission spectrum according to Georganopoulos et al. (2001), who included the effects of the beaming and the KN cross section, because our interest is in the application of our model to blazars. We first solve equation (1) without the term of electron escape to compare with the results with the escape term. In Figure 1 we show the electron spectra for different values of  $\gamma_{\max}$  and  $p = 2$  and  $1.8$  ( $p = 1.8$  was used in our model of 3C 279; Kusunose et al. 2003). In this figure,  $n_{\text{soft}}(x) = n_0 \delta(x - x_0)$  and  $x_0 m_e c^2 = 1.25$  keV, where  $\delta$  is the Dirac delta function; when the bulk Lorentz factor of the jet is  $\Gamma = 25$ , this soft photon energy is 50 eV in the frame of the soft photon source. The value of  $q_0$  is chosen to set the injection rate of electrons to  $1 \text{ cm}^{-3} \text{ s}^{-1}$ , and the value of  $n_0$  is fixed to set the energy density of soft photons to  $8.3 \times 10^{-2} \text{ ergs cm}^{-3}$ ; this value of the energy density corresponds to  $1.3 \times 10^{-4} \text{ ergs cm}^{-3}$  in the frame of the soft photon source if  $\Gamma = 25$ . When  $p = 2$ ,  $n_e(\gamma) \propto \gamma^{-3}$  for  $\gamma x_0 \lesssim 0.1$ , i.e., scattering occurs in the Thomson regime. The KN effects appear for  $\gamma x_0 \gtrsim 0.1$ , and the electron spectra become harder. For example, when  $\gamma_{\max} = 10^6$ ,  $n_e(\gamma) \propto \gamma^{-1.3}$  for  $p = 2$  and  $10 < \gamma x_0 < 10^3$ , with a prominent peak at  $\gamma x_0 \sim 3 \times 10^3$ . It should be noted that if we solve equation (1) at the lower energy region down to  $\gamma = 1$ , the electron spectrum should have an infinite peak at  $\gamma = 1$  because of cooling. Since

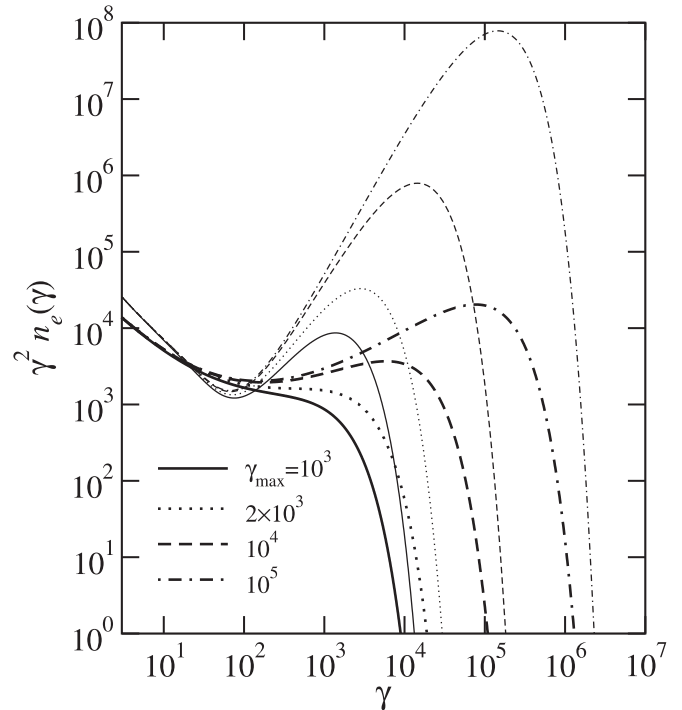


FIG. 2.—Electron spectra calculated with the KN cross section (*thick lines*) and with the Thomson approximation (*thin lines*). Injected electrons obey a power law with  $p = 2$ , and the external soft photons follow a blackbody distribution with a temperature of 1.25 keV.

we solved equation (1) at large values of  $\gamma$ , this peak does not appear in the figures.

The deviation of the Thomson approximation (eq. [11]) from the KN formulation (eq. [1]) is shown in Figure 2. Here the injected soft photons obey the Planck distribution with a temperature of 1.25 keV and an energy density of  $8.3 \times 10^{-2} \text{ ergs cm}^{-3}$ . The values of  $n_e(\gamma)$  are different from those in Figure 1, because the external soft photon spectra are different. Since electrons with  $\gamma > 3/(4x)$  do not suffer from cooling in the Thomson approximation, a large number of electrons stay in the high-energy region. Thus, just assuming that the cross section vanishes for  $\gamma > 3/(4x)$  considerably overestimates the number density of electrons in the high-energy region. More accurate treatments are needed to properly estimate the high-energy electron spectrum.

The observed photon spectra emitted by the electrons with  $p = 2$  shown in Figure 1 are presented in Figure 3 (the spectra from electrons with  $p = 1.8$  given in Fig. 1 are shown in Fig. 4). It is assumed that the emission region is in the moving blob with  $\Gamma = 25$  at redshift  $z = 0.538$  (the redshift of 3C 279) and that the size of the emission region is  $R = 7 \times 10^{17} \text{ cm}$  (the blob size appropriate for 3C 279 in our model; Kusunose et al. 2003). The soft photon spectrum of the external photon source is monochromatic, with energy  $x_0 m_e c^2 = 1.25$  keV. Although the scattering cross section decreases owing to the KN effects for  $\gamma \gtrsim 0.1x_0^{-1}$ , there are still ample hard photons to be observed. In these figures synchrotron spectra with  $B = 0.3$  G are also shown. The energy density of the magnetic field is  $3.6 \times 10^{-3} \text{ ergs cm}^{-3}$ , which is to be compared with the soft photon energy density of  $8.3 \times 10^{-2} \text{ ergs cm}^{-3}$ . It is clear that when  $\gamma_{\max}$  increases, the synchrotron luminosity also increases. On the other hand, the Compton luminosity does not, because of inefficient cooling in the KN regime. Thus, if the Compton cooling occurs mainly in the KN regime, the dominance of the synchrotron luminosity

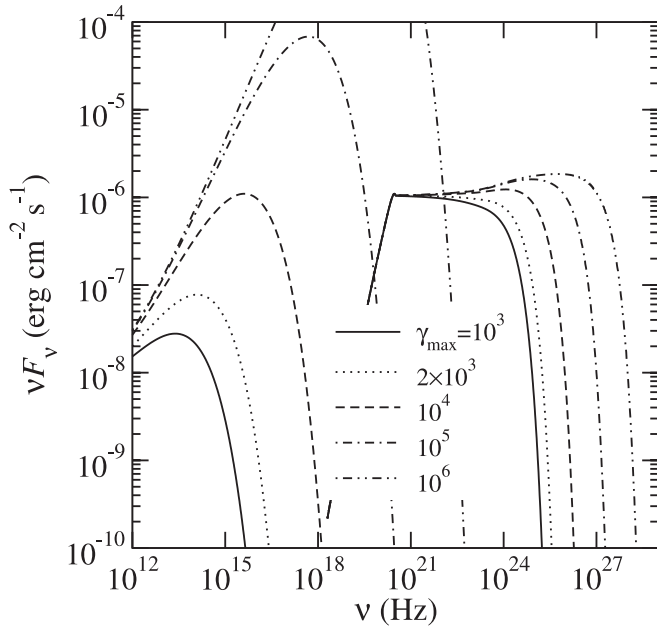


FIG. 3.—Photon spectra emitted by electrons shown in Fig. 1 with  $p = 2$  and various values of  $\gamma_{\max}$ . The spectra are shown in the observer's frame. The curves on the right are the emission by IC scattering, and the curves on the left are by synchrotron radiation with  $B = 0.3$  G.

over the Compton luminosity does not mean that the magnetic energy density dominates other energy contents, such as external soft photons. It should be noted that the cooling rate of synchrotron emission is not taken into account in the electron kinetic equation and that the synchrotron spectra are shown only for the purpose of seeing the effect of different shapes of the electron spectra in the high-energy region. For  $\gamma_{\max} \gtrsim 10^3$ , the synchrotron cooling dominates the Compton cooling when the magnetic field is fixed at 0.3 G. On the other hand, if  $B \sim 0.02$  G, the synchrotron cooling time is one tenth of the Compton cooling time for  $\gamma \lesssim 10^5$ .

As mentioned above, we solved equation (1) at large values of  $\gamma$ . If we solve the equation at small values of  $\gamma$  down to 1,

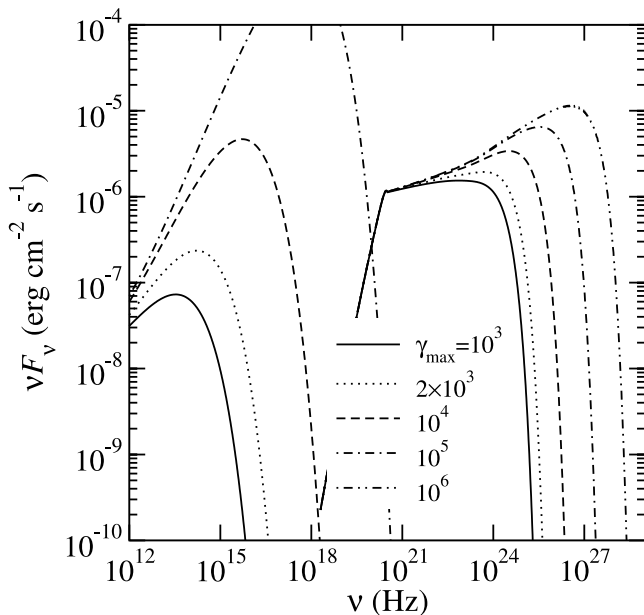


FIG. 4.—Same as Fig. 3, except  $p = 1.8$ .

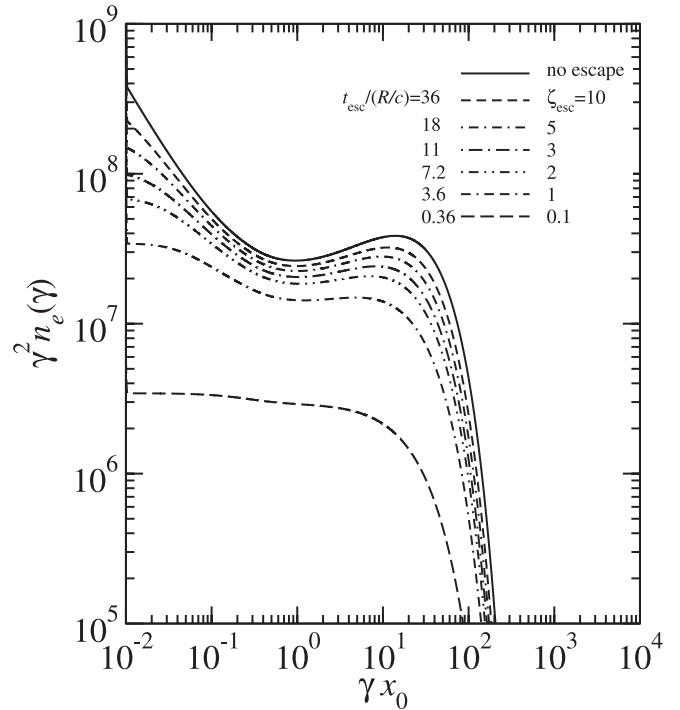


FIG. 5.—Electron spectra with various values of escape time;  $\gamma_{\max} = 10^4$  and  $p = 2$  are assumed for the injection spectrum of electrons. The soft photons are monochromatic with energy 1.25 keV. From upper to lower curves,  $\zeta_{\text{esc}} = \infty$  (no escape), 10, 5, 3, 2, 1, and 0.1.

there should be an infinite number of electrons at  $\gamma = 1$ , and they should produce a peak at  $h\nu \sim \Gamma^2 h\nu_0 \sim 31$  keV in the photon spectrum, where  $h\nu_0$  is the soft photon energy in the rest frame of the soft photon source: 50 eV in our numerical calculations.

From Figures 3 and 4 it is found that the small differences in the electron spectrum caused by the different values of  $\gamma_{\max}$  result in different values of the power-law index of the lower energy part of the synchrotron spectrum, or the part of the spectrum below the synchrotron peak energy. This might be used to determine observationally the KN effects on the electron spectrum by observations in radio through optical bands.

The electron spectrum in the jet with electron escape from the emission region is shown in Figure 5 for the different values of  $\zeta_{\text{esc}}$ , assuming that the soft photons are monochromatic. In this figure,  $\gamma_{\max} = 10^4$ ,  $p = 2$ , and  $m_e c^2 x_0 = 1.25$  keV are assumed. We assumed that  $\zeta_{\text{esc}} \propto t_{\text{esc}}$ , and  $\zeta_{\text{esc}} = 1$  corresponds to  $t_{\text{esc}} = 3.6R/c$  for the adopted parameter values. When the escape time is shorter, the electron density decreases, the spectrum becomes flatter, and the peak energy of the bump decreases. When  $\zeta_{\text{esc}} = 0.1$ , the shape of the electron spectrum is almost the same as that of the injected electrons. The electron spectra for the different values of  $\gamma_{\max}$  are shown in Figure 6 with  $\zeta_{\text{esc}} = 1$ . Even when the electron escape time is a few times the light crossing time ( $R/c$ ), the energy density of high-energy electrons with  $\gamma > x_0^{-1}$  is still large, and the emission from those electrons is expected to be as shown below.

The electron spectra with the Thomson approximation and those with the KN cross section are compared in Figure 7. The injected soft photons follow a blackbody distribution with a temperature of  $kT = 1.25$  keV and an energy density of  $8.3 \times 10^{-2}$  ergs  $\text{cm}^{-3}$ . As with the case in which there is no electron escape, the Thomson approximation results in more electrons in the high-energy region than the calculations with the KN cross

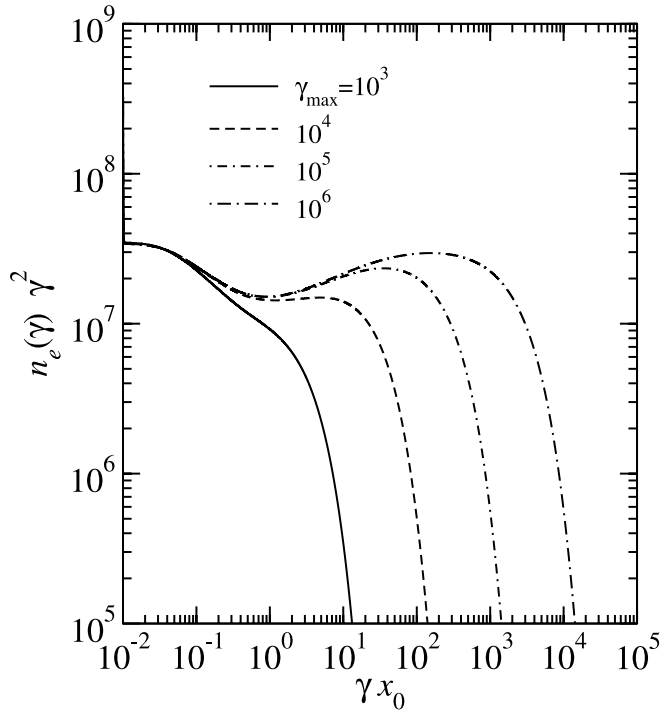


FIG. 6.—Same as Fig. 5, but for  $\zeta_{\text{esc}} = 1$  and the various values of  $\gamma_{\text{max}}$ .

section. In the Thomson approximation there is a dip at  $\gamma \sim 100$ , which corresponds to  $\gamma kT/(m_e c^2) \approx 0.24$ .

The photon spectra from the jet with electron escape are shown in Figures 8 and 9. In both figures, the external soft photons are monochromatic. Synchrotron emission with  $B = 0.3$  G is also shown for comparison with the IC emission. In Figure 8,  $\gamma_{\text{max}} = 10^4$ ,  $p = 2$ , and various values of  $\zeta_{\text{esc}}$  are assumed. When  $\zeta_{\text{esc}} = 0.1$ , the Compton luminosity is higher than

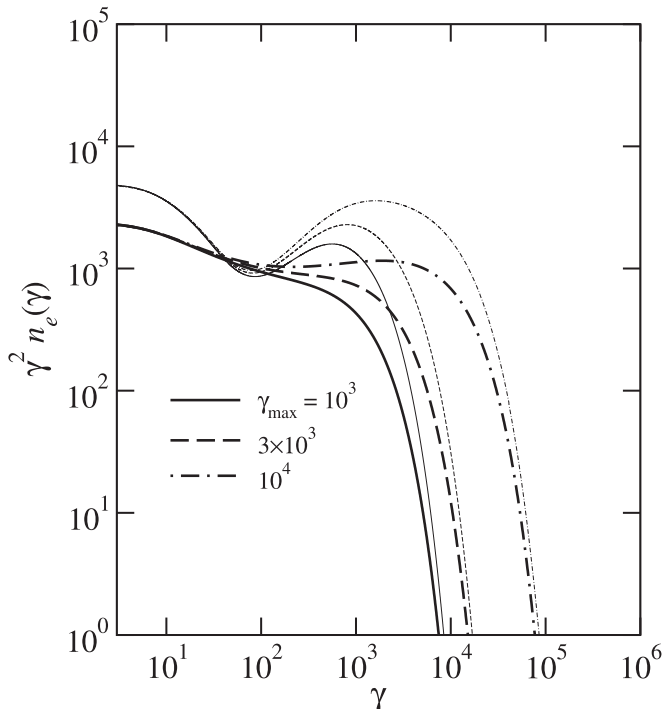


FIG. 7.—Electron spectra with escape calculated with the KN cross section (thick lines) compared with those calculated by the Thomson approximation (thin lines). Electron escape time is  $t_{\text{esc}} = 1.5 \times 10^3$  s, which corresponds to  $\zeta_{\text{esc}} = 1$  for the KN case.

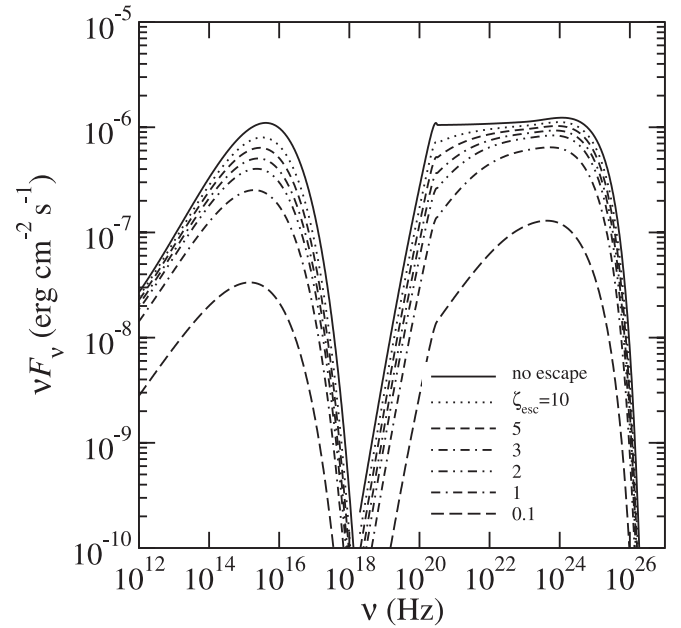


FIG. 8.—Photon spectra emitted by the electrons shown in Fig. 5. Curves on the left are by synchrotron radiation with  $B = 0.3$  G, and curves on the right are by IC scattering.

the synchrotron luminosity. When  $\zeta_{\text{esc}}$  increases, both the Compton and synchrotron luminosities increase, while the spectral shape of both components changes as a result of the change in the electron energy distribution due to the KN effects. In Figure 9,  $\zeta_{\text{esc}} = 1$ ,  $p = 2$ , and different values of  $\gamma_{\text{max}}$  are assumed. It is found that the peak of  $\nu F_\nu$  of the Compton spectrum occurs at  $h\nu \sim 10^3 m_e c^2$  for large enough values of  $\gamma_{\text{max}}$  ( $\geq 10^4$ ) when  $\zeta_{\text{esc}} = 1$ . When  $\zeta_{\text{esc}}$  is larger, the peak of  $\nu F_\nu$  occurs at a slightly larger value of photon energy. The peak energy  $h\nu \sim 10^3 m_e c^2$  is due to the electrons with  $\gamma \sim 160$ , i.e.,  $\gamma x_0 \sim 0.4$ , which scatter seed photons in the Thomson regime producing photons with energy  $\sim \gamma^2 x_0 m_e c^2$ . Taking into account  $z = 0.538$  and  $\Gamma = 25$ , the observed peak energy appears at  $h\nu \sim 10^3 m_e c^2$ .

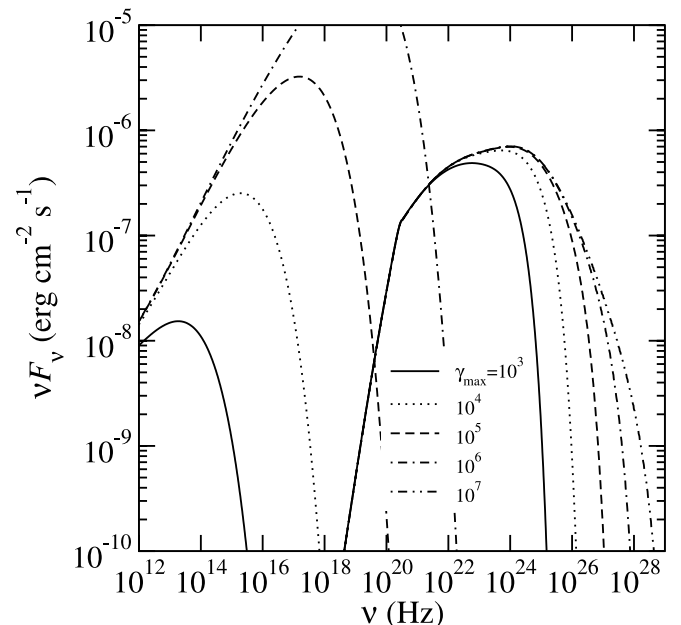


FIG. 9.—Photon spectra emitted by the electrons shown in Fig. 6 ( $\zeta_{\text{esc}} = 1$ ) produced by IC scattering and synchrotron radiation with  $B = 0.3$  G.

Because the synchrotron luminosity is larger than the Compton luminosity for  $\gamma_{\max} \gtrsim$  a few  $\times 10^4$ , the properties of electron and photon spectra described here for  $\gamma_{\max} \gtrsim$  a few  $\times 10^4$  are correct when  $B$  is smaller than 0.3 G to keep the synchrotron luminosity below the Compton luminosity.

#### 4. SUMMARY

We studied the effects of inverse Compton (IC) scattering in the Klein-Nishina (KN) regime, paying attention to its application to the gamma-ray emission from blazars. For this purpose we solved the kinetic equation of electrons with electron escape, assuming that electron cooling occurs predominantly by IC scattering of external soft photons. The photon spectrum was calculated, assuming that the emitting region is moving relativistically along the line of sight, i.e., emission from a relativistic jet is considered. The seed soft photons of IC scattering are assumed to come from external sources. Because of the Doppler effect, the energy of the seed photons is higher for electrons in the jet. Then the KN effects appear for smaller values of  $\gamma$  compared with electrons in a stationary emitting region. In our numerical calculations, the bulk Lorentz factor is set to be 25, and the seed soft photon energy is 50 eV in the frame of the soft photon source, which is based on our model of 3C 279 (Kusunose et al. 2003). For these parameters, electrons with  $\gamma > 400$  scatter soft photons in the KN regime.

When the escape of electrons can be neglected compared with the cooling, the electron spectrum becomes harder than the injection spectrum for  $\gamma > x_0^{-1}$ , as Blumenthal (1971) showed,

because of the less efficient cooling in the KN regime. Although the cooling rate is smaller compared with that in the Thomson regime, gamma rays with an energy of  $\sim \gamma_{\max}$  are amply emitted by IC scattering. When electron escape is taken into account, the number of high-energy electrons decreases. However, gamma rays in GeV region are still emitted by IC scattering.

In astrophysical objects such as blazars, where IC scattering is a major radiative process, the spectrum of nonthermal electrons needs to be carefully considered. Although a simple power-law spectrum of electrons might fit the observed emission spectrum, it may not represent the physical conditions in the source. The self-consistent treatment of photons and particles should be taken into account. We finally remark on the effects of synchrotron radiation and synchrotron self-Compton scattering on the electron spectrum. When the magnetic field is strong enough, these processes decrease the number density of electrons with very large Lorentz factors, and the upturn in the high-energy tail of the electron spectrum becomes less prominent. This effect was included in our previous paper (Kusunose et al. 2003), where the KN effects are still apparent in the electron spectrum.

This work has been partially supported by Scientific Research Grants (M. K.: 15037210; F. T.: 14079205 and 16540215) from the Ministry of Education, Culture, Sports, Science and Technology of Japan.

#### REFERENCES

- Blumenthal, G. R. 1971, *Phys. Rev. D*, 3, 2308  
 Blumenthal, G. R., & Gould, R. J. 1970, *Rev. Mod. Phys.*, 42, 237  
 Coppi, P. S., & Blandford, R. D. 1990, *MNRAS*, 245, 453  
 Dermer, C. D., & Schlickeiser, R. 1993, *ApJ*, 416, 458  
 Georganopoulos, M., Kirk, J. G., & Mastichiadis, A. 2001, *ApJ*, 561, 111 (erratum 604, 479 [2004])  
 Ghisellini, G., Maraschi, L., & Dondi, L. 1996, *A&AS*, 120, 503  
 Inoue, S., & Takahara, F. 1996, *ApJ*, 463, 555  
 Jones, F. C. 1968, *Phys. Rev.*, 167, 1159  
 Kusunose, M., Takahara, F., & Kato, T. 2003, *ApJ*, 592, L5  
 Lightman, A. P., & Zdziarski, A. A. 1987, *ApJ*, 319, 643  
 Mücke, A., Protheroe, R. J., Engel, R., Rachen, J. P., & Stanev, T. 2003, *Astropart. Phys.*, 18, 593  
 Rybicki, G. B., & Lightman, A. P. 1979, *Radiative Processes in Astrophysics* (New York: Wiley)  
 Sikora, M., Begelman, M. C., & Rees, M. J. 1994, *ApJ*, 421, 153  
 Zdziarski, A. A. 1988, *ApJ*, 335, 786  
 ———. 1989, *ApJ*, 342, 1108  
 Zdziarski, A. A., & Krolik, J. H. 1993, *ApJ*, 409, L33